Material Profile Influences in Bulk-Heterojunctions

John D. Roehling,[1] Christopher W. Rochester,[1] Hyun Wook Ro,[2] Peng Wang,[3] Jaroslaw Majewski,[3] K. Joost Batenburg,[4,5] Ilke Arslan,[6] Dean M. Delongchamp,[2] Adam J. Moulé[1]

[1]Department of Chemical Engineering and Materials Science, University of California, Davis, California
[2]Materials Science and Engineering Laboratory, National Institute of Standards and Technology (NIST), Gaithersburg, Maryland
[3]Lujan Neutron Scattering Center, Los Alamos National Laboratory (LANL), Los Alamos, New Mexico
[4]Scientific Computing, Centrum Wiskunde and Informatica, Amsterdam, Netherlands
[5]iMinds-Vision Lab, University of Antwerp, Antwerp, Belgium
[6]Fundamental and Computational Sciences, Pacific Northwest National Laboratory (PNNL), Richland, Washington
Correspondence to: A. J. Moulé (E-mail: amoule@ucdavis.edu)

Received 22 May 2014; revised 15 July 2014; accepted 17 July 2014; published online 6 August 2014
DOI: 10.1002/polb.23564

ABSTRACT: The morphology in mixed bulk-heterojunction films are compared using three different quantitative measurement techniques. We compare the vertical composition changes using high-angle annular dark-field scanning transmission electron microscopy with electron tomography and neutron and x-ray reflectometry. The three measurement techniques yield qualitatively comparable vertical concentration measurements. The presence of a metal cathode during thermal annealing is observed to alter the fullerene concentration throughout the thickness of the film for all measurements. However, the absolute vertical concentration of fullerene is quantitatively different for the three measurements. The origin of the quantitative measurement differences is discussed. © 2014 Wiley Periodicals, Inc. J. Polym. Sci., Part B: Polym. Phys. **2014**, *52*, 1291–1300

KEYWORDS: blends; bulk-heterojunction; electron microscopy; miscibility; morphology; structure; vertical-segregation

INTRODUCTION Thin films of phase separated mixtures of polymer:fullerenes known as bulk-heterojunctions (BHJs) have long demonstrated their potential as high-performance organic photovoltaic materials. Structural studies of BHJs have determined that local molecular ordering strongly influences many characteristic properties of the film.[1,2] Achieving the optimized domain-size, mutual-miscibility, and domain connectivity have been shown to be of principal importance in optimizing a given material system.[3–9] However, the morphology perpendicular to the substrate plane is typically not well characterized. As this is the direction of charge transport, it seems there is a gap in the understanding of how morphology can affect characteristic device properties. Recently, increased attention has been given to the vertical profile of the materials in a device, but conflicting results of the measured material profile are common.[10–14] This is likely due to differences in sample preparation, but also to the uncertainties in the measurements themselves and over-interpretation of the extracted profiles.

The surface energy of the substrate has been shown to strongly affect the vertical material profile.[15–20] Both the orientation of polymer chains and distribution of materials can change based on their interactions with the underlying substrate.[1] Recently, neutron (NR) reflectometry measurements have shown that a metal cathode, capping the BHJ film during annealing, also affects the vertical material distribution within the BHJ.[15] In a 1:1 by weight poly(3-hexylthiophene):-phenyl-C_{61}-butyric acid methyl ester (P3HT:PC_{61}BM) BHJ film, enrichment of the fullerene component at both interfaces occurs upon thermal annealing in a metal capped film. With no capping metal, only enrichment at the substrate interface occurs (and to a lesser degree) and a polymer skin layer is reported to form at the air interface.[14] NR is the only measurement technique which can measure through the metal electrode. Without the metal present, it is not possible to distinguish between the P3HT skin layer and the sample's surface roughness. We compare several measurement techniques here to remove the uncertainty associated with data fitting, sample geometry, or contrast within the sample.

Additional Supporting Information may be found in the online version of this article.

© 2014 Wiley Periodicals, Inc.

The most widely used tool to measure vertical material profiles is reflectometry, either NR or x-ray reflectometry (XRR). Typically only one of these techniques is used for characterization, but as this work will demonstrate, it is difficult to obtain absolute quantitative results by relying upon a single measurement technique. Moreover, the accuracy of the extracted profile strongly depends upon the quality of the data acquired, as well as the uniqueness of the fit. The quality of the data can be affected by sample quality, such as in-plane inhomogeneities, sample flatness, surface roughness, and differences in the beam footprint. These can all affect the accuracy of the fitted profile. Here, we compare the results of three separate techniques measuring the same samples* and observe quantitative differences between each measurement technique [The samples for the NR and XRR were the exact same physical samples, but separate samples were necessary for electron tomography (ET), these were made with identical preparation conditions.] The uncertainties within each technique are discussed and compared. The quantitative differences observed demonstrate that techniques utilizing under-determined solutions to fit measured data (which all three techniques used are) must be interpreted with care, the use of multiple measurements together is recommended for the most reliable quantitative results.

One difficulty with measuring P3HT:PCBM BHJ mixtures is that the components lack the necessary contrast for many measurements. X-ray reflectometry, ET, and visible light ellipsometry are all difficult to use quantitatively because of this fact. We therefore turned to the use of endohedral fullerenes which provide much better contrast compared to PCBM for x-rays and electrons. By utilizing $Lu_3N@C_{80}$-PCBEH in lieu of PCBM, we are able to perform NR, XRR, and ET with sufficient contrast to compare the results of vertical profile measurements. High-angle annular dark-field scanning transmission electron microscopy with ET is performed using the discrete algebraic reconstruction technique (DART) for increased accuracy.[21–24] The advantage of using ET over reflectometry is that three phases can be distinguished as well as in-plane morphology information. An increase in mixed-phase presence at the substrate interface is observed in samples heated with a metal cap present. NR and XRR are not able to distinguish mixed and pure phases within the same volume.

EXPERIMENTAL

Sample Preparation

The samples prepared for NR and XRR were 10:13 and 10:19 by weight P3HT:$Lu_3N@C_{80}$-PCBEH (65 kDa from Plextronics and from Luna Innovations Inc., respectively) solutions in chlorobenzene, spin-cast on Si wafers with a native oxide (solution was held at 60 °C until deposition to achieve a smooth surface). The samples were then placed in a thermal evaporator and 40 nm of Ca was deposited. The samples were then annealed on a hot plate at 150 °C for 5 min. After heating the Ca was removed with a generous amount of deionized water. The entire preparation was done within a nitrogen atmosphere. These exact physical samples were measured using both NR and XRR.

For ET, the samples had to be prepared such that the BHJ layer could be removed from the substrate, so they could be picked up by a TEM grid. For this purpose, poly(3,4-ethylenedioxythiophene): poly(styrenesulfonate) (PEDOT:PSS) was used as a sacrificial layer. PEDOT:PSS was first spin-cast onto glass substrates in air at 2500 RPM for 60 s, then heated for 5 min at 110 °C and transferred into a nitrogen glove-box. A 20 mg/mL solution of P3HT:$Lu_3N@C_{80}$-PCBEH was subsequently spin-cast onto the substrate at 60 °C at 1000 RPM. Two of the three ET samples (the Ca capped films) were placed into a thermal evaporation chamber and 40 nm of Ca was deposited. All three films were then annealed at 150 °C for 5 min. The Ca capped films were then washed with water as done with the NR/XRR samples. The films were then scratched to obtain a small section and this was subsequently floated off in water and transferred onto 200 mesh lacey carbon TEM grids for imaging.

NR Measurement

NR measurements were performed using the Surface Profile Analysis Reflectometer (SPEAR) at the Lujan Neutron Scattering Center at Los Alamos National Laboratory. The NR beam is obtained from a spallation source and after moderation by liquid H_2. The wavelength on SPEAR used neutrons ranged from 4.5 to 16 Å. Specular reflection is recorded by a position-sensitive time-of-flight (ToF) detector. Reflectivity is then calculated as the ratio of the intensity of the reflected beam to the incident beam. In a ToF instrument, the neutron's momentum, and therefore its wavelength, is determined by measuring the time it takes the neutron to travel the length of the instrument. During the NR experiment, neutrons impinge on a sample at a small angle, θ, and the ratio of elastically scattered to incident neutrons is measured. This ratio is defined as the reflectivity, R, and is measured as a function of the momentum transfer vector, Q. In case of specular reflection, $Q_z = 4\pi\sin(\theta)/\lambda$.

The analysis of data obtained from a single incident angle provides a limited Q_z range. Therefore, our NR measurements were performed at three different incident angles ($\theta = \sim 0.5$, 1.0, and 2.6°, respectively) to gain a maximum usable Q_z range of about 0.25 Å^{-1}. Analysis of specular reflectometry data provides information regarding the coherent scattering length density (SLD) distribution normal to a samples surface. SLD is a value uniquely determined by the physical and chemical nature of a material. The resulted SLD profile is essentially the chemical/density distribution profile as a function of depth perpendicular to the sample surface.

XRR Measurement

Specular XRR measurements were performed on a Philips XPERT diffractometer using Cu-Kα X-ray radiation ($\lambda = 1.5418$ Å). The incident beam is focused with a curved mirror into a 4 bounce Ge [220] crystal monochromator before being incident onto the sample. The reflected beam is further conditioned with a 3-bounce Ge [220] crystal monochromator

ensure the specular condition. The angular reproducibility of the goniometers that control the sample rotation and angular position of X-ray detector was 0.0001°. The reflectivity was collected at 25 °C under vacuum for all samples. The footprint length was varied in the range of (5–35) mm during XRR measurement.

ET Measurement

The tilt series used for reconstruction were performed on a JEOL 2100 F at 200 kV. A minimum of ±65° was recorded for each sample in 1° increments. Reconstructions were performed using the DART and three gray levels. Film thicknesses were measured via a surface profilometer and subsequently used in the reconstructions. The locations of the top and bottom of the film had to be manually selected (keeping the measured thickness). Film shrinkage was assumed to be negligible and was difficult to measure experimentally due to some build up of surface contamination (see Supporting Information for how this was dealt with). Gray levels were selected based on those which minimized the difference between the forward projected reconstruction and the original images (i.e., projection error). The gray levels selected correspond to pure P3HT regions, mixed P3HT/fullerene regions, and fullerene-rich regions.[21] More details on the imaging and reconstruction process are given in the Supporting Information and Refs. 21 and 22.

RESULTS AND DISCUSSION

To obtain quantitative results from a fitting technique, constraints must be placed upon the fit, which force compliance with mass-conservation. All of the fits used in this work are constrained so the volume percentage of the components corresponds to the mass input of the samples (see Supporting Information for more details). The SLD and density of the pure components must therefore must be known. A density of 1.1 and 2.07 g/cm^3 were used for P3HT and $Lu_3N@C_{80}$-PCBEH, respectively. The latter was back calculated from the measured XRR SLD of a pure, spin-cast film. Using this measured density, the NR SLD of pure $Lu_3N@C_{80}$-PCBEH was calculated (see Supporting Information). In these analyses, zero volume change due to mixing is implicitly assumed.

First, to confirm that enrichment of fullerene at the interfaces occurs when the films are heated with a metal electrode present, vertical concentration profiles (VCPs) were extracted from ET measurements. Figure 1 shows the measured VCP of fullerene as a function of normalized film thickness for different films and measurement techniques. The left-hand side of the plot corresponds to the top of the film (either the metal or air interface) and the right-hand side of the plot corresponds to the substrate interface. Comparing the ET measurements [Fig. 1(b)] with previously extracted profiles from 1:1 by weight P3HT:PCBM mixtures [Fig. 1(a)], a similar enrichment of fullerene at both interfaces can be observed. A similar qualitative shape is observed in both measured samples, the double hump of the uncapped sample is reproduced in the ET profile as well as increased fullerene content at the interfaces is observed in all the capped samples.

Without further measurement one might attribute the above quantitative differences to the fact that there are different fullerenes present. Figure 1(a) shows P3HT/PCBM BHJ samples while Figure 1(b) shows a mixture of P3HT with $Lu_3N@C_{80}$-PCBEH. But measurement of similarly prepared samples with two other quantitative techniques illustrates other possibilities. Figure 1(c,d) show the same two P3HT/$Lu_3N@C_{80}$-PCBEH samples measured with NR and XRR. There are clear quantitative differences between the NR and XRR profiles. Recall that these were the exact same physical samples measured with both NR and XRR. Clearly, some degree of uncertainty exists in these measured profiles.

For the 10:13 sample, the top interface has about a 10% difference in fullerene content, but the buried interface measures about 15% higher in the XRR profile and rapidly decays toward the center of the film. For the 10:19 film, the NR measures a higher fullerene content at the top interface and the buried interface decays rapidly toward the center. Additionally, the level of fullerene in the center of the 10:13 film is about 5% different, where a 15% difference is present in the 10:19 film. The drop in the concentration at the top surface seen in the reflectometry profiles is likely due to surface roughness, not from a P3HT skin, but for these measurements the determination cannot be made. Lastly, the XRR profiles exhibit larger fullerene content at the buried interface, where the NR profiles show larger fullerene content at the top interface. These vertical fit profiles all minimized the χ^2 error between theory and measurement and yet are vastly different between the two techniques. With the fitting differences in the NR and XRR VCP profiles, the ET measurements now seem less likely to be from quantitative differences in actual VCP, but from some sort of measurement bias. We will now discuss some of the differences in the measurements, sample preparation, fitting procedures, and cause of uncertainties.

Sample and Measurement Uncertainties

Clearly, the three measurements of the P3HT:$Lu_3N@C_{80}$-PCBEH are qualitatively the same. The 10:19 sample has increased fullerene content at the top interface compared with the 10:13 samples, and all have increased fullerene content at the substrate interface. Hence, the trend is the same in all three measurements, what are the causes of the differences? At this point, we will belabor technical details of the sample preparation to illustrate how different measurement techniques can be difficult to quantitatively compare and why certain sample preparation conditions were chosen. Important technical details of the sample preparation are:

1. A Si/SiO_2 substrate was used without PEDOT:PSS for NR and XRR measurements because PEDOT:PSS increases the roughness of both the top surface and the substrate interface. The increased roughness makes obtaining a unique fit to the data more difficult.
2. For ET measurement the samples were prepared with a PEDOT:PSS substrate because a water permeable layer is needed to remove the BHJ layer.

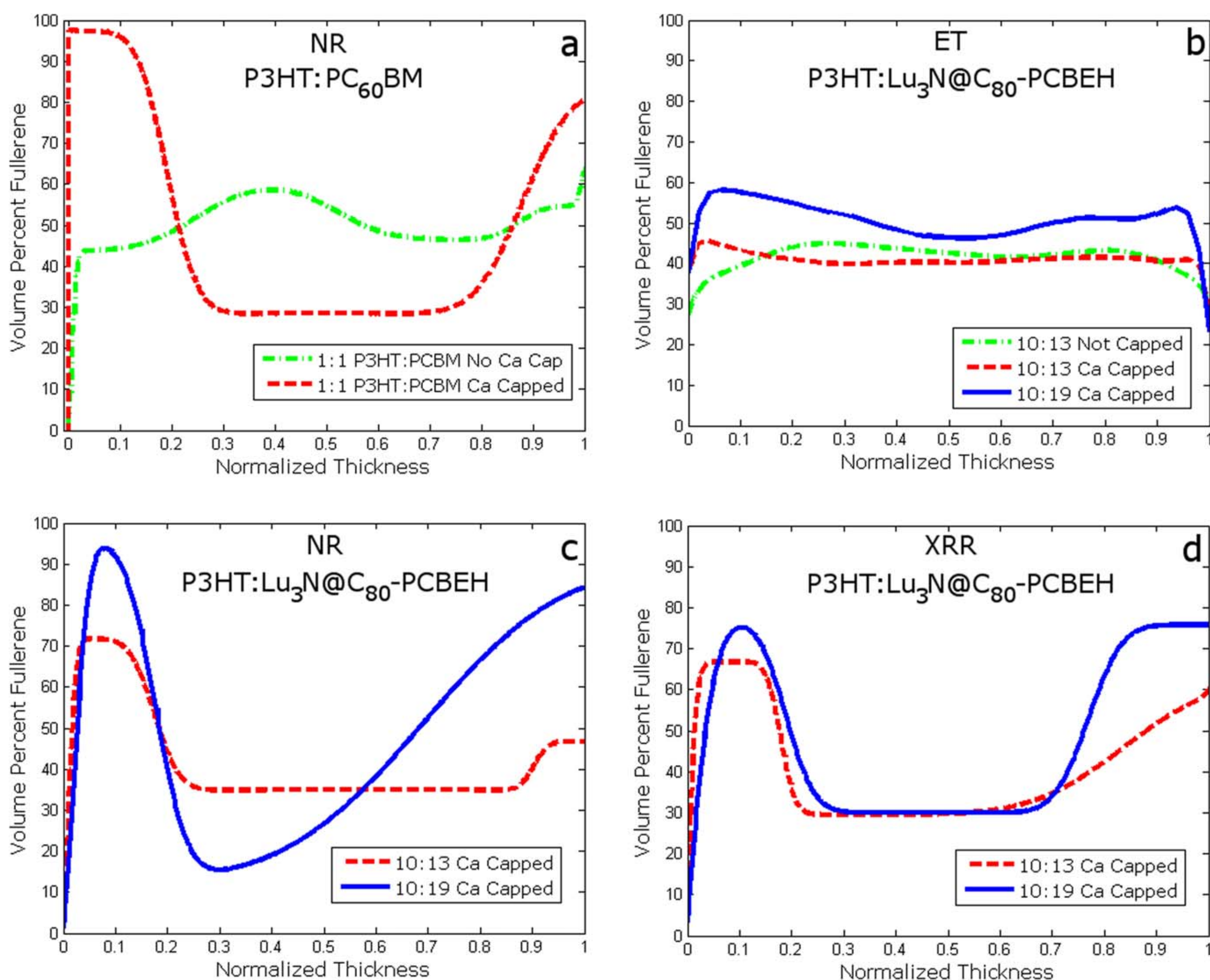

FIGURE 1 NR profile of thermally annealed 1:1 (by weight) P3HT:PC$_{61}$BM films heated with and without a metal cap present (a). (Reproduced from Ref. [15] with permission.) VCP of the three P3HT:Lu$_3$N@C$_{80}$-PCBEH films measured by ET (b). NR profile of P3HT:Lu$_3$N@C$_{80}$-PCBEH films (c). XRR profile of P3HT:Lu$_3$N@C$_{80}$-PCBEH films (d). The left-hand side (zero) corresponds to the top surface of the films and the right-hand side (one) corresponds to the substrate in all plots. [Color figure can be viewed in the online issue, which is available at wileyonlinelibrary.com.]

3. The Ca layer had to be removed prior to ET and XRR measurement because the Ca strongly absorbs electrons and x-rays.
4. The Ca was also removed prior to NR measurement because it oxidizes in air, creating sample roughness. We later found that Ag or Al metal cap can be left on the sample and the uniqueness of the NR fit improves greatly. However, since we required removing the metal for ET measurement, we chose to remove it for comparison with the other techniques as well.

The difference between the reflectometry and ET measurements could have resulted simply because the substrates were different. This could alter the profile since the surface energies are not identical. However, the difference between the NR and XRR measurement fits cannot be for this reason, as they are measurements of identical samples (but with different beam footprints, as will be discussed later). One clear difference between measurements is the sample area probed. ET samples the smallest area with about 1.5 μm^2 the unit should be square micrometers (area not length). By comparison, XRR samples a larger area on the order of several mm^2 and several cm^2 for NR. So, although the samples were identical, the sampled areas were different and this could have a large impact on the data if the films were not homogeneous over the four inch Si substrate. In a more detailed look at the effect of inhomogeneities of the tomographic data, we sub-sampled the tomographic data sets in 280 $\times$ 280 nm^2 sections. The difference in most morphological parameters measured was $\pm$5%, showing that the film is relatively homogenous.[25] This would likely be true for larger areas as well, however, in the tomographic data any large fullerene

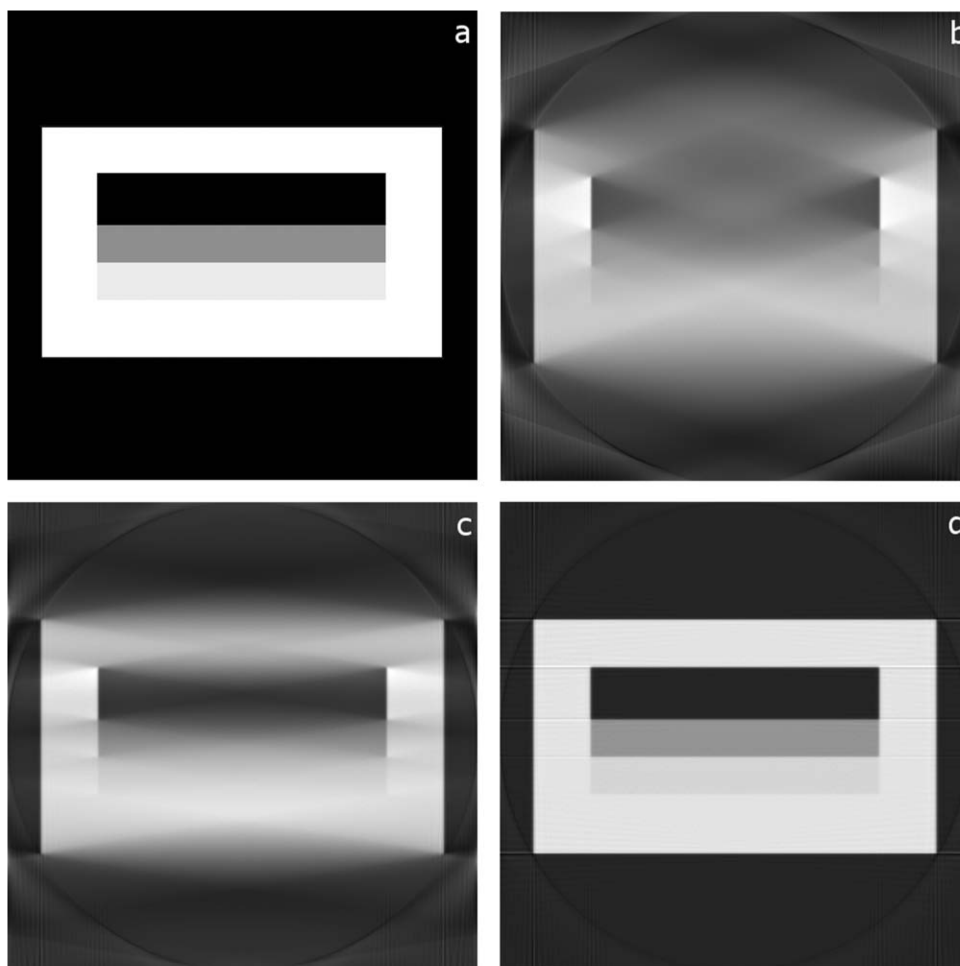

FIGURE 2 SIRT reconstructions of a slab object. The original (a) is shown as well as reconstructions of the same image with projections taken at different tilt ranges to illustrate the effect of an incomplete tilt range: $\pm 70^\circ$ (b), $\pm 80^\circ$ (c), and $\pm 90^\circ$ (d); 200 iterations were used for these examples.

agglomerates were avoided in the measurement out of necessity, whereas completely avoiding fullerene aggregates' effects in the reflectometry data is not possible. Discussion of this point in more detail is continued below in section "Reflectometry."

Another effect is the composition of the films. Due to the small quantities of the endohedral fullerene available, the films have an uncertainty in the actual composition of ± 0.1 (ratio $Lu_3N@C_{80}$-PCBEH:P3HT). This is due to the resolution of the weighing scale (± 0.1 mg), which was used for the solution preparation. This uncertainty affects the calculated volume percent fullerene of the ET profiles and reflectometry profiles by about $\pm 5\%$.

Electron Tomography

ET and reflectometry measurements are acquired in orthogonal geometries. Samples for reflectometry are films on a substrate that are probed at low incident angle while samples for ET are unsupported films that contact the electron beam at $90^\circ \pm 65^\circ$ incidence (with 90° being normal to the surface). The result is that reflectometry is more sensitive to information in the vertical plane of the film while ET is much more sensitive to features in the lateral plane of the film. ET cannot perfectly reconstruct a 3D film volume because information is missing from tilt angles at low incidence angle to the film.[26] Figure 2 illustrates the effect of missing angles by reconstructing a slab of three different gray values using the simultaneous iterative reconstruction technique (SIRT, a subroutine of DART). More information is gained in the reconstructed object about the original object when a higher tilt range is used to probe its volume. DART is an improved numerical reconstruction technique that can recover a more accurate image from an under sampled volume (see Ref. 24 for details of reduced elongation), but some information may still be lost. Since our tilt series were acquired with a maximum tilt range of $\pm 70^\circ$, this is certainly a contributing factor. It must be noted that the elongation of the reconstructions shown in Figure 2 are much greater than would be obtained in our reconstructions utilizing DART, Figure 2 is simply shown to illustrate the effect of the missing wedge.

An additional feature, which makes the exact quantification of the VCP difficult by ET is the geometry which must be

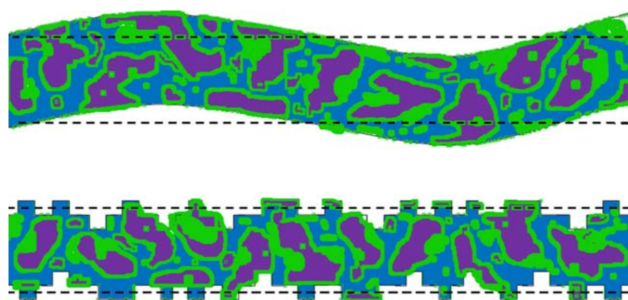

FIGURE 3 The effect of thickness/surface undulations and the assumed film boundaries (dotted line) as well as the effect of surface roughness is illustrated (greatly exaggerated). Errors in the exact film boundaries would result in a smearing out of the VCP calculated from ET. [Color figure can be viewed in the online issue, which is available at wileyonlinelibrary.com.]

assumed by the reconstruction process. To obtain accurate information from the DART algorithm for this type of sample, the film must be assumed to be a flat slab with smooth parallel sides (a more detailed description of the process is included in the Supporting Information). In reality, slight deviations from this can be present such as surface roughness or wrinkles in the film. Any of these features are lost in the assumed geometry. This is illustrated in Figure 3. Avoiding these artifacts is quite difficult because these types of features are not able to be seen when collecting the tilt-series. Any roughness and undulations in the thickness will result in a smearing out of the VC profile, which is what is seen in the ET data (compared with the reflectometry profiles). We estimate the roughness of the film (in the area measured for ET) to be ~5 nm [The surface roughness of P3HT:PCBM films has been reported to be from a few nm up to ~10 nm, depending on processing.[4,27] The roughness of films in this study were comparable (data not shown)].

Additional measurement uncertainties come from the gray level selection. Ideally, the gray level for the pure materials would be measured separately and used as inputs, then only the mixed phase gray level would be fit. This would ensure further accuracy, but unfortunately it is not possible to prepare a homogeneous film of amorphous P3HT: $Lu_3@NC_{80}$PCBEH that would have a density and mixing ratio that is identical to the mixed domains between crystalline–P3HT and $Lu_3@NC_{80}$PCBEH–rich domains. Despite these shortcomings the overall trend of the vertical profile from ET is qualitatively consistent with other measurements; hence, it is certainly sensitive to changes in the vertical profile. Most importantly local morphology information is also available through ET and the contribution of each phase to the vertical profile can be explored, something not possible using NR or XRR. This will be explored further in section "Additional information extracted from ET."

Reflectometry

In contrast to ET, reflectometry techniques are much more sensitive to density or concentration changes in the vertical direction and average over a large enough area so that effects of thickness undulations and surface roughness are averaged out. However, to get accurate information from reflectometry, knowledge of the correct model to be used in the fitting process is needed. Multiple profiles and models can result in very similar "goodness of fit" (χ^2). This was certainly observed when performing fits on these data. Although overall the shape of the fits extracted were similar for the lowest achievable χ^2 values, it was certainly possible to add more layers and achieve slightly lower χ^2. Similarly, the χ^2 could be lowered by considering nonphysical mass distributions/ratios.

The quality of the collected data has a very large effect on the extracted profile. The quality is largely affected by the sample itself. For these samples, NR revealed that the 4 diameter Si wafer had a slight bow, resulting in significant increase in the spread of the reflected beam as observed in the 2D detector. To mitigate this problem only the central part of the specular reflection was taken into account during the data reduction. This procedure is equivalent to selecting much smaller footprint of the NR beam on the sample and therefore is less sensitive to sample bending and possible, long-length, sample in-plane inhomogeneities.

Despite data reduction, the sample area on which the NR beam impinges is still much larger than that with XRR. Since there is a small angular distribution in the beam the interaction length of the beam with the sample is longer in the direction of the beam (~4 cm for NR and ~5 mm for XRR). In the reflectometry samples, we observed areas which seemed to contain large fullerene aggregates. Therefore, obtaining data from an area which was completely free of these aggregates with NR was not likely. However, since the interaction area is much smaller in XRR the sample was able to be positioned so the inclusion of these areas was less likely. This is one possible explanation for part of the discrepancy in the extracted profiles. Our attempts to fit both datasets simultaneously did not yield acceptable results; this is most likely due to the differences in measured area (beam footprint).

A final note regarding reflectometry data is that NR has the capability to measure to a higher Q/Q_c, where Q_c is critical momentum vector. This makes it more susceptible to roughness and since it measures over a larger area, it is more accurate for homogenous samples. However, in the case of these samples, with the observed in-plane inhomogeneities, we believe that the XRR profile is more representative of the true profile.

The extracted profiles have a larger discrepancy than might be expected for the measurement of the same samples. We therefore make the recommendation that multiple measurements of the same samples be performed in order to ensure that the extracted profiles are reliable. Moreover, use of a second technique can serve as an error-check, and help identify less-reliable data, as in this case with the NR data.

Sample Stability

We have stated that the same sample was used for both NR and XRR. There was >2 months of time between the measurements. It is reasonable to ask whether the samples might

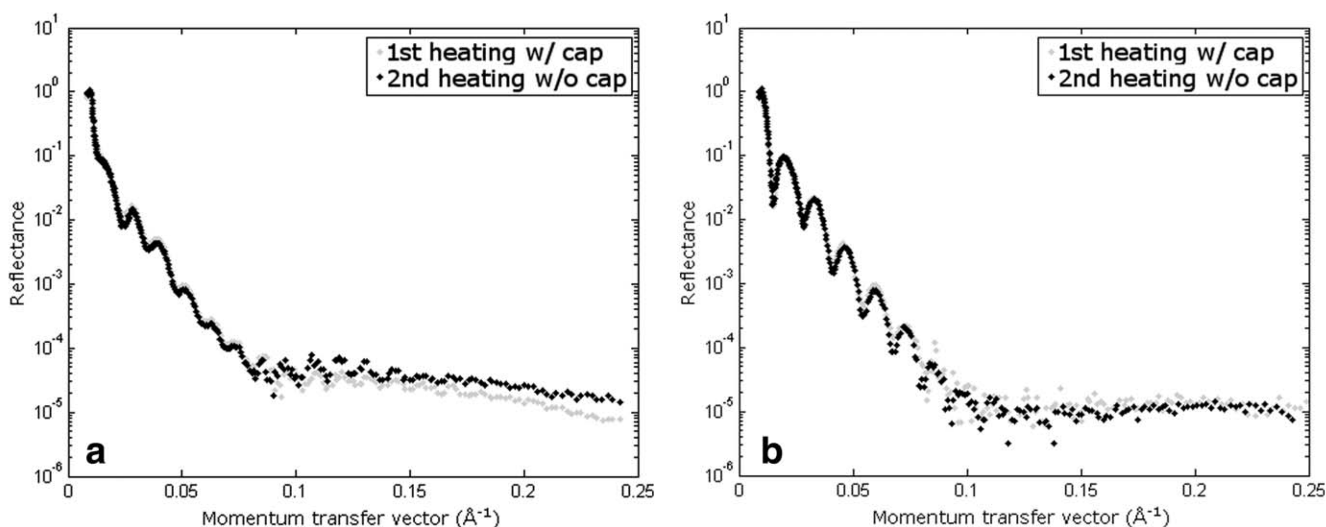

FIGURE 4 NR data of both the 10:13 (a) and 10:19 samples (b), after the first heating with the metal cap present, and the second heating with the metal cap removed.

have changed in that time. Unfortunately, this question cannot be answered with NR and XRR on this sample. But, a measurement of the thermal stability of the sample was made. NR data was collected twice for both reflectometry samples. First, as stated in the "Experimental" section, the sample was heated with the Ca electrode present, the electrode was then removed, and the sample was measured with NR. Next, the sample was heated a second time at 150 °C for 5 min after the Ca electrode had been removed (it was heated in air), and then NR was measured a second time. Our hypothesis, at the time, was that the P3HT and fullerene would change vertical configuration to match the heated in air (not capped) sample shown in Figure 1(a).

The NR data (Fig. 4) shows that the reflectance is practically identical after the second heating. This demonstrates that once the sample has been heated and the P3HT and $Lu_3N@C_{80}$-PCBEH domains have formed, the components have found thermodynamically stable positions and the barrier to diffusion is raised, so the VCP can become "locked in." Even for large values of momentum transfer there is virtually no difference in the reflectance, which we would expect to see with the establishment of a P3HT skin layer at the sample surface. It must be noted that this may not be true for all polymer:fullerene mixtures. In our previous work on P3HT:$Lu_3N@C_{80}$-PCBEH morphology[21] it was observed that this mixture is very thermally stable even after being solvent annealed at high temperatures for extended periods of time. This was attributed to the fact that the $Lu_3N@C_{80}$-PCBEH fullerene does not crystallize and so diffusion due to Ostwald ripening is not observed.[21] Hence, we hypothesize that blends of noncrystallizing fullerene with crystallizing polymers are much more likely to have stable VCPs than blends of crystallizing fullerenes with polymers.

Additional Information Extracted from ET

The ET measurements, unlike the reflectometry measurements, also allow for more detailed investigation of the vertical profile through examining individual phases. Figure 5 shows the volume percentage of each phase as a function of the vertical position. This plot shows the local percentage of each phase at a particular slice through the film volume (at each measured position, the total volume at each slice is 100%).

The fullerene-rich phase shows enrichment at the Ca electrode in both the capped samples. This was shown to be caused by the higher surface energy of the fullerene selectively moving to the high energy surface.[15–18] The fullerene-rich phase also shows a decrease at both interfaces in the uncapped sample. The increase in fullerene content at the interfaces is consistent with the reflectometry measurements made here and in other measurements.[10,13–15,19,20,28] The presence of the metal seems to affect not only the composition at the metal interface, but also the substrate interface. The exact reason for this is unclear but it has implications for device function. The increase in fullerene phase volume seen at the interfaces of the capped films compared to the uncapped film would likely result in improved electron transport to the electrodes for these films. The increase in fullerene phase volume seen at the interfaces of the capped films compared to the uncapped film would likely result in improved electron transport to the electrodes for these films. The presence of more fullerene at the cathode has been shown to increase charge selectivity.[29] It has also been shown that heating with a capping metal electrode increases the power conversion efficiency more than heating before capping.[8] This was attributed to the metal electrode making better contact with the film and reducing the resistance, but it could also be contributed to by vertical segregation effects enhancing selectivity at the cathode.

The mixed phase in the capped samples is enriched at the PEDOT:PSS electrode relative to the uncapped sample. This largely contributes to the increase of fullerene concentration at this interface (relative, compared with the uncapped). The increase in mixed phase concentration likely results from a

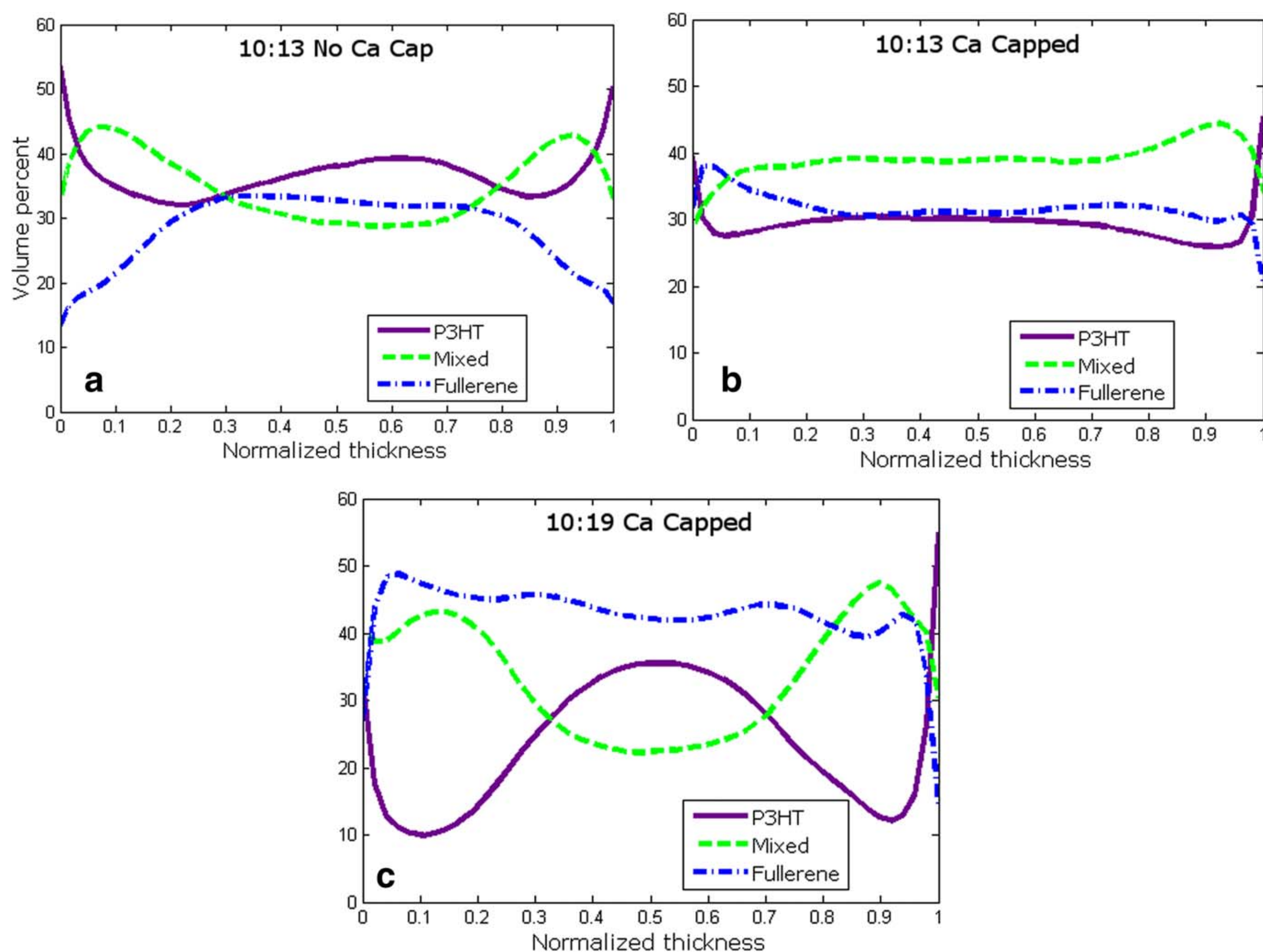

FIGURE 5 Vertical phase profile of the three films measured by ET, 10:13 w/o a Ca cap (a), 10:13 w/ a Ca cap (b), and 10:19 w/ a Ca cap (c). The plots are normalized to the thickness of each film. The left-hand side (zero) corresponds to the top surface of the films and the right-hand side (one) corresponds to the substrate in all plots. [Color figure can be viewed in the online issue, which is available at wileyonlinelibrary.com.]

combination of undetermined capping metal effects and the mixing of P3HT with PSS at the PEDOT:PSS interface.[30] Here, the P3HT chains would be more likely to be in an amorphous conformation with some which have undergone a redox reaction. Previous studies of P3HT:$PC_{61}BM$ devices have shown that there is reduced photocurrent generation near this interface.[31,32] This data demonstrates that reduced photo-current generation is possibly contributed to by vertical segregation effects, where more amorphous P3HT:fullerene mixture is present near the substrate causing reduced charge mobility and reduced light absorption in the red.[33,34] Increased recombination rates and charged P3HT traps states quenching excitons could also contribute to the reduced photocurrent generation observed.[31,35]

The P3HT phase has a dip in local concentration near the electrodes in all three films. The rapid sharp increase in pure P3HT concentration within 3–4 nm ($\sim$0.05 of the normalized thickness) of the interface is due to a reconstruction artifact. This artifact comes from a smoothing step which reduces the gray level of all pixels at the extreme edges, causing more P3HT to be thresholded in the final volume at the top and bottom of the film. This step effectively flattens the features shown in Figure 2. We chose not to remove this artifact to avoid the possibility of altering other features in the reconstruction. It only affects the very edge voxels and has a minor effect on the overall composition. P3HT seems to aggregate preferentially away from the interfaces.

The decreased presence of the P3HT phase near the interfaces could be attributed to excluded volume effects. The interfaces reduce the available motion of P3HT chains, making it more difficult for the chains to order themselves. In the 10:19 film the pure P3HT volume is about 10% near the interfaces. Hole transport would likely suffer in these regions in the film.

The fraction of pure P3HT domains to total P3HT is about 45% in both the Ca capped samples, but is about 60% in the uncapped sample. This suggests that the metal surface reduces overall P3HT aggregation. The relatively large

difference between the surface energy of the P3HT and the metal could cause this, making the P3HT minimize contact, which minimizes the likelihood of a pure phase at the interface. However, this could again be attributed in part to excluded volume effects, where reduced available motion makes it more difficult for the P3HT chains to aggregate.

CONCLUSIONS

The VCP of films of P3HT:$Lu_3N@C_{80}-$PCBEH were measured using three separate quantitative techniques. The results from each technique were, to some extent, different when the data from a single technique was considered. Despite measuring the same physical samples, the profiles extracted from NR and XRR did not quantitatively align. This is likely due to a number of factors; (i) the probed sample area is different, (ii) differences in sample preparation, and (iii) uncertainties within the extracted profile. The differences between the reflectometry profiles can be mostly attributed to differences in beam footprint and sample inhomogeneities. The ET profile seemed to be smeared out, in comparison to the reflectometry profiles, which can be attributed to missing information and limitations of the reconstruction algorithm, assumptions of the film boundaries, and uncertainties due to sample preparation differences. However, the overall trend of the ET was similar to reflectometry measurements, demonstrating that it is certainly sensitive to vertical profile changes. Additionally, ET data can contain local morphology and phase information, which is not possible with reflectometry methods.

These results demonstrates that the measured morphology of different films should not be assumed to be equivalent unless the fabrication conditions and measurement conditions are, indeed, equivalent. Additionally, multiple measurements of the same sample are necessary to ensure that extracted VCPs are accurate. Simultaneous fitting of multiple datasets is the best way to ensure that an accurate quantitative profile is extracted. This was not possible in this case, but separate techniques enabled problems with one dataset to be identified, which might not have otherwise been found.

In conclusion, over-interpretation of "quantitative" data is something which researchers need to be cautious of. We have shown that measurements of the same samples can result in markedly different extracted profiles and that quantitative information is difficult to determine absolutely. These data demonstrate the need to verify extracted profiles using multiple types of measurements and to fully understand the nature of the data, without over-interpretation.

ACKNOWLEDGMENTS

The authors thank Luna Innovations, Inc. for donating the endohedral fullerenes used in this study and Plextronics for the P3HT. They are gratefully thank the National Science Foundation Energy for Sustainability Program, Award No. 0933435. This work benefited from the use of the Lujan Neutron Scattering Center at Los Alamos Neutron Science Center funded by the DOE Office of Basic Energy Sciences and Los Alamos National Laboratory under DOE Contract DE-AC52-06NA25396. This research was also supported in part by Laboratory Directed Research & Development program at PNNL. The Pacific Northwest National Laboratory is operated by Battelle for the US Department of Energy under contract DE-AC05-76RL01830.

REFERENCES AND NOTES

1 A. Salleo, R. J. Kline, D. M. DeLongchamp, M. L. Chabinyc, *Adv. Mater.* **2010**, *22*, 3812–3838.

2 C. H. Woo, B. C. Thompson, B. J. Kim, M. F. Toney, J. M. J. Frechet, *J. Am. Chem. Soc.* **2008**, *130*, 16324–16329.

3 D. Chirvase, J. Parisi, J. C. Hummelen, V. Dyakonov, *Nanotechnology* **2004**, *15*, 1317–1323.

4 G. Li, V. Shrotriya, J. Huang, Y. Yao, T. Moriarty, K. Emery, Y. Yang, *Nat. Mater.* **2005**, *4*, 864–868.

5 M. Reyes-Reyes, K. Kim, D. L. Carroll, *Appl. Phys. Lett.* **2005**, 87, 083506–083506-3.

6 A. J. Moulé, K. Meerholz, *Adv. Funct. Mater.* **2009**, *19*, 3028–3036.

7 A. J. Moulé, K. Meerholz, *Adv. Mater.* **2008**, *20*, 240–245.

8 W. L. Ma, C. Y. Yang, X. Gong, K. Lee, and A. J. Heeger, *Adv. Funct. Mater.* **2005**, *15*, 1617–1622.

9 D. R. Kozub, K. Vakhshouri, L. M. Orme, C. Wang, A. Hexemer, E. D. Gomez, *Macromolecules* **2011**, *44*, 5722–5726.

10 M. Shao, J. Keum, J. Chen, Y. He, W. Chen, J. F. Browning, J. Jakowski, B. G. Sumpter, I. N. Ivanov, Y.-Z. Ma, C. M. Rouleau, S. C. Smith, D. B. Geohegan, K. Hong, K. Xiao, *Nat. Commun.* **2014**, *5*.

11 H.-J. Liu, U.-S. Jeng, N. L. Yamada, A.-C. Su, W.-R. Wu, C.-J. Su, S.-J. Lin, K.-H. Wei, M.-Y. Chiu, *Soft Matter* **2011**, *7*, 9276–9282.

12 S. B. Kirschner, N. P. Smith, K. A. Wepasnick, H. E. Katz, B. J. Kirby, J. A. Borchers, D. H. Reich, *J. Mater. Chem.* **2012**, *22*, 4364–4370.

13 J. W. Kiel, M. E. Mackay, B. J. Kirby, B. B. Maranville, C. F. Majkrzak, *J. Chem. Phys.* **2010**, *133*, 074902.

14 D. M. DeLongchamp, R. J. Kline, A. Herzing, *Energy Environ. Sci.* **2012**, *5*, 5980–5993.

15 S. A. Mauger, L. Chang, S. Friedrich, C. W. Rochester, D. M. Huang, P. Wang, A. Moulé, *Adv. Funct. Mater.* **2013**, *23*, 1935–1946.

16 D. Chen, F. Liu, C. Wang, A. Nakahara, T. P. Russell, *Nano Lett.* **2011**, *11*, 2071–2078.

17 M. Campoy-Quiles, T. Ferenczi, T. Agostinelli, P. G. Etchegoin, Y. Kim, T. D. Anthopoulos, P. N. Stavrinou, D. D. C. Bradley, J. Nelson, *Nat. Mater.* **2008**, *7*, 158–164.

18 Z. Xu, L.-M. Chen, G. Yang, C.-H. Huang, J. Hou, Y. Wu, G. Li, C.-S. Hsu, Y. Yang, *Adv. Funct. Mater.* **2009**, *19*, 1227–1234.

19 D. S. Germack, C. K. Chan, R. J. Kline, D. A. Fischer, D. J. Gundlach, M. F. Toney, L. J. Richter, D. M. DeLongchamp, *Macromolecules* **2010**, *43*, 3828–3836.

20 D. S. Germack, C. K. Chan, B. H. Hamadani, L. J. Richter, D. A. Fischer, D. J. Gundlach, D. M. DeLongchamp, *Appl. Phys. Lett.* **2009**, *94*, 233303–233303-3.

21 J. D. Roehling, K. J. Batenburg, B. F. Francis, I. Arslan, A. J. Moulé, *Adv. Funct. Mater.* **2013**, *23*, 2115–2122.

22 K. J. Batenburg, J. Sijbers, *IEEE Trans. Image Process.* **2011**, *20*, 2542–2553.

23 S. Bals, K. J. Batenburg, J. Verbeeck, J. Sijbers, G. Van Tendeloo, *Nano Lett.* **2007**, *7*, 3669–3674.

24 K. J. Batenburg, S. Bals, J. Sijbers, C. Kuebel, P. A. Midgley, J. C. Hernandez, U. Kaiser, E. R. Encina, E. A. Coronado, G. Van Tendeloo, *Ultramicroscopy* **2009**, *109*, 730–740.

25 O. Wodo, J. D. Roehling, B. Ganapathysubramanian, A. J. Moulé, *Energy Environ. Sci.* **2013**, *6*, 3060–3070.

26 P. Midgley, M. Weyland, *Ultramicroscopy* **2003**, *96*, 413–431.

27 G. Li, Y. Yao, H. Yang, V. Shrotriya, G. Yang, Y. Yang, *Adv. Funct. Mater.* **2007**, *17*, 1636–1644.

28 C. He, D. S. Germack, R. Joseph Kline, D. M. Delongchamp, D. A. Fischer, C. R. Snyder, M. F. Toney, J. G. Kushmerick, L. J. Richter, *Sol. Energy Mater. Sol. Cells* **2011**, *95*, 1375–1381.

29 A. Guerrero, B. Drling, T. Ripolles-Sanchis, M. Aghamohammadi, E. Barrena, M. Campoy-Quiles, G. Garcia-Belmonte, *ACS Nano* **2013**, *7*, 4637–4646.

30 D. M. Huang, S. A. Mauger, S. Friedrich, S. J. George, D. Dumitriu-LaGrange, S. Yoon, A. J. Moulé, *Adv. Funct. Mater.* **2011**, *21*, 1657–1665.

31 A. J. Moulé, K. Meerholz, *Appl. Phys. B* **2008**, *92*, 209–218.

32 G. F. Burkhard, E. T. Hoke, S. R. Scully, M. D. McGehee, *Nano Lett.* **2009**, *9*, 4037–4041.

33 A. Moulé, J. Bonekamp, K. Meerholz, *J. Appl. Phys.* **2006**, *100*, 094503.

34 A. Moulé, K. Meerholz, *Appl. Phys. B* **2007**, *86*, 771–777.

35 A. J. Ferguson, N. Kopidakis, S. E. Shaheen, G. Rumbles, *J. Phys. Chem. C* **2008**, *112*, 9865–9871.